BIOSYSTEMS ENGINEERING 143 (2016) 79–94

Available online at www.sciencedirect.com

ScienceDirect

journal homepage: www.elsevier.com/locate/issn/15375110

Research Paper

Reducing air pollution with hybrid-powered robotic tractors for precision agriculture

Mariano Gonzalez-de-Soto [a,b,*,1,2], *Luis Emmi* [a,1], *Carmen Benavides* [b,2], *Isaias Garcia* [b,2], *Pablo Gonzalez-de-Santos* [a,**,1]

[a] *Centre for Automation and Robotics (UPM-CSIC), Ctra CAMPO REAL km 0,2, 28500 Arganda del Rey, Madrid, Spain*

[b] *Escuela de Ingenierías Industrial e Informática, Universidad de León, Dept. de Ingeniería Eléctrica y de Sistemas y Automática, Campus de Vegazana s/n, 24071, León, Spain*

ARTICLE INFO

Article history:
Received 7 August 2015
Received in revised form
8 January 2016
Accepted 20 January 2016
Published online 6 February 2016

Keywords:
Atmospheric emissions
Exhaust gasses
Hybrid power
Robotic tractor
Precision agriculture

A hybrid energy system used in robotic tractors for precision weed and pest control in agriculture is evaluated and its exhaust emissions compared with the use of an internal combustion engine as a single power source. The agricultural implements require power for hydraulic pumps and fans which, initially, was provided by a power take-off system (PTO), wasting a lot of energy. The objectives of this work were to design and assess a hybrid energy system including the removal of the alternators from the tractor and the modification of the agricultural implements to replace the PTO power with electric power, using small pumps and small fans. These changes improved energy use and reduced the atmospheric pollution emission from the internal combustion engine. The hybrid energy system used the original combustion engine of the tractor in combination with a new electrical energy system, which consisted of a hydrogen fuel cell. An analysis of the exhaust gases using the internal combustion engine as the single power source and using the hybrid energy system was carried out to compare the results obtained. The results showed a reduction in emissions of almost 50% for the best case.

1. Introduction

Non-road vehicles, such as agricultural machines, use large amounts of energy, usually fossil fuels and emit large amounts of pollution to atmosphere. Off-road internal combustion engines (ICEs) emit carbon dioxide (CO_2), nitrogen oxides (NO_X), carbon monoxide (CO), particulate matters (PM) and hydrocarbon (HC). CO_2 and NO_X are greenhouse gases, and they contribute to global warming. Furthermore, they can

* Corresponding author. Centre for Automation and Robotics (UPM-CSIC), Ctra CAMPO REAL km 0,2, 28500 Arganda del Rey, Madrid, Spain.

** Corresponding author.

E-mail addresses: mariano.gonzalez@car.upm-csic.es (M. Gonzalez-de-Soto), luis.emmi@car.upm-csic.es (L. Emmi), carmen.benavides@unileon.es (C. Benavides), isaias.garcia@unileon.es (I. Garcia), pablo.gonzalez@car.upm-csic.es (P. Gonzalez-de-Santos).

1 Tel./fax: +34650015576; +34689876367; + 34918711900x221.

2 Tel./fax: +34650015576; +34987291000x5395; +34987291000x5289.

http://dx.doi.org/10.1016/j.biosystemseng.2016.01.008

List of symbols and acronyms

CO	Carbon monoxide
CO_2	Carbon dioxide
D	Implement draft force (kN)
E_{EES}	Energy demand supplied by the electrical energy system (kW h)
EES	Electrical energy system
E_{ICE}	Energy demand supplied by the internal combustion engine (kW h)
EMS	Energy management system
GPS	Global positioning system
HC	Hydrocarbon
HES	Hybrid energy system
HFC	Hydrogen fuel cell
ICE	Internal combustion engine
MR	Motion resistance (kN)
n	Number of tools
NO_X	Nitrogen oxides
P_{EES}	Power demand supplied by the electrical energy system (kW)
PEM	Proton exchange membrane
P_{ICE}	Power demand supplied by the internal combustion engine (kW)
$P_{IMP\ control}$	Electrical power of the implement control system (kW)
PM	Particulate matter
P_{Task}	Electrical power demand of the task (kW)
PTO	Power take-off
P_{Tool}	Electrical power of each implement tool (kW)
$P_{UGV\ control}$	Electrical power of the UGV control system (kW)
PV	Photovoltaic
PVGIS	Photovoltaic geographical information system
RDS	Row detection system
RTK	Real time kinematic
SFC_V	Specific fuel consumption volume (l kW h^{-1})
SHC	Specific hydrogen consumption (kg kW h^{-1})
TE	Total energy (kW h)
TPH	Three-point hitch
UGV	Unmanned ground vehicle
WDS	Weed detection system

cause health problems: NO_X may cause or worsen respiratory diseases, such as bronchitis or emphysema, and may also aggravate existing heart disease; CO binds to haemoglobin in the blood and can cause harmful health effects by reducing oxygen delivery to the body's tissues and organs (such as the brain and heart), reducing work capacity and mental skills; decreasing learning ability; causing headaches, nausea, and dizziness; and, at extremely high levels, can cause death. HCs are volatile organic compounds, such as xylenes, toluene, benzene and ethyl-benzene. These compounds can cause headaches, dizziness, loss of consciousness, etc. Furthermore, benzene is carcinogenic and increases the likelihood of leukaemia. Particle matter (PM) emitted from combustion engines is a complex mixture of liquid droplets and fine particles have a number of components, including sulphates and nitrates, metals, organic chemicals, and dust or soil particles. These particles can also affect the lungs or heart function causing serious health problems according to the US Environmental Protection Agency (EPA, 2015).

Some research analysing energy use and the pollution emitted by agricultural tractors has been carried out. Clements et al. (1995) analysed the energy used in weed control using herbicides and tillage and found that alternative weed control strategies can provide interesting energy savings. Hansson, Lindgren, and Norén (2001) compared different methods and calculated the average absolute and specific emission values from agricultural tractors. Considering the consequences of these emissions, we need to progressively reduce the use of hydrocarbon fuels. To achieve this, fossil fuels can be replaced by cleaner fuels or electrical systems. Dalgaard, Halberg, and Porter (2001) presented a model of fossil fuel use for Denmark and proposed the use of their model to simulate possible agricultural production scenarios in an effort to improve future techniques. Guzman and Alonso (2008) analysed energy use in Mediterranean agriculture and evaluated the contribution of the organic olive oil production towards improving energy efficiency and compared the results with respect to the conventional production. Soni, Taewichit, and Salokhe (2013) presented an analysis of the CO_2 emissions and energy consumption in agricultural task performed over rain fed crops. Peltre, Nyord, Bruun, Jensen, and Magid (2015) analysed how increasing soil organic carbon content decreased the draft force in ploughing and the consequent reductions in fuel consumption and emissions.

To date much research has studied alternative energy sources to the use of fossil fuels and ICEs. Biofuel is one of these alternatives. Gasparatos, Stromberg, and Takeuchi (2011), analysed the impact of biofuels on society and environment demonstrating that biofuels generate many impacts that must be considered. However, many works on alternative power sources propose the use of batteries; for example, Delucchi and Lipman (2001) analysed the lifecycle costs of battery-powered electric vehicles (that is, initial vehicle cost as well as operating and maintenance costs) to develop a detailed model of the lifecycle costs of electric vehicles. This model was compared to a gasoline ICE vehicle model and determined the battery properties needed to reduce the costs of electric vehicles to be economically competitive with ICE vehicles. Mousazadeh et al. (2010) looked at the various battery technologies available for use in solar-assisted plug-in hybrid electric tractors to be used in light-duty agricultural operations. This was extended by Mousazadeh et al. (2011) who carried out a life cycle analysis of a solar-assisted plug-in hybrid electric tractor and compared the results with that of a similar power output ICE tractor considering economic costs and environmental emissions. They determined that the life cycle costs of solar-assisted plug-in hybrid electric tractors are lower than those of ICEs.

Other important alternatives to batteries as the energy source in electric vehicles are fuel cells; usually, the same fuel can also be used by an ICE. For example, Mulloney (1993) proposed the use of environmentally benign fuel cells for power production, avoiding the use of fossil fuels for field crop production and distribution. They also presented an engineering systems analysis of how such systems can mitigate pollution. Lutz, Larson, and Keller (2002) compared the theoretical maximum efficiency of a fuel cell to the efficiency of a Carnot cycle using the same fuel to determine the net reaction. They found that the maximum efficiency was quite similar in both systems, but in practice, a fuel cell exhibits higher efficiency because ICEs cannot operate at theoretical maximum efficiency. This would require a very high temperature, which would generate problems in terms of engine construction materials. Eaves and Eaves (2004), compared the manufacturing and refuelling costs of a fuel cell vehicle and a battery electric vehicle using an automobile model reflecting the largest segment of light-duty vehicles. They determined that a battery electric vehicle performs far more favourably in terms of cost, energy efficiency, mass, and volume. In another example of this type of researchy, Offer, Howey, Contestabile, Clague, and Brandon (2010) compared battery electric vehicles, hydrogen fuel cell electric vehicles and hydrogen fuel cell plug-in hybrid vehicles. They concluded that battery electric vehicles and hydrogen fuel cell plug-in hybrid vehicles have reasonably similar lifecycle costs. However, these costs are higher than the costs of ICEs (in 2010) but these costs could drop by 2030. These vehicles offer different advantages depending on driving pattern.

The approach presented in this paper was tested using agricultural autonomous vehicles developed within the RHEA project (http://www.rhea-project.eu/). During the development of this project, it was observed that during precision agriculture tasks, the ICE very frequently supplied more power than needed, particularly when the implement (a tool or utensil for doing work (Dictionary, 2015), in this case, agricultural work) uses PTO power. Thus, the objective of this work was to develop, implement and assess a hybrid energy system (HES) for robotic tractors used in precision agriculture. These agricultural vehicles were designed to work at low speed; thus, the aerodynamics and vehicle size do not present substantial problems. Furthermore, in many agriculture tasks the tractor needs to counterweight or increase its weight. Therefore, weight is usually not a problem. Taking advantage of these features, the proposed energy system combines the use of batteries, a hydrogen fuel cell, and photovoltaic (PV) cells with the original ICE of the tractor to achieve a substantial decrease in fossil fuel use and a consequent reduction in the emission of pollutants. This energy system allowed the tractor to increase the work capacity because the implement can incorporate its own motor decreasing the workload of the ICE of the tractor.

To carry out this work, the main objective was divided into the following sub-objectives:

- Analyse the main features of the used systems (Section 2.1).
- Implement an energy model to predict the energy requirements (Section 2.2).
- Analyse the energy demands of each subsystem and task (Section 3.1.1)
- Design and implement an HES that supplies the energy requirements of all of the different agriculture tasks accomplished (Section 3.1.2).
- Present the results obtained after conducting a series of field experiments to check the energy system and assess the pollutant emission reduction, comparing HES with the system based on the ICE (Section 3.2).

2. Materials and methodology

This section presents the system used and its main power features, focussing on obtaining an energy model. The aim was to develop a model that would allow the energy requirements of three agricultural tasks considered in this work to be analysed (weed control on fire-resistant crops with wide furrows, weed control on herbaceous crops and pest control in tree crops). According to the energy requirements, as system was designed and the size of the energy system specified.

2.1. *Systems*

In this work, an unmanned ground vehicle (UGV) and three different implements, one for each of agricultural tasks analysed were used. Here, the main features of this UGV are presented. It had a control system, an energy system and a fuel consumption measurement system. The system and the method used to measure the fuel consumption and estimate the exhaust gases from the ICE are described. The agricultural tasks and implements used in this work are presented; that is, a description of the changes in the implements to replace the PTO power by electric power as well as an enumeration of the implement power features, which were needed to design the energy model.

2.1.1. *Unmanned ground vehicle*

The UGV used in this work is based on the commercial vehicle CNHi Boomer 3050 CVT compact tractor. It inherits the main features from the original tractor that was modified and programmed using a special software package. The UGV was improved with an additional power system; a control system, which manages the main vehicle functions; and a safety system, which provides safety to the vehicle, the environment and the people involved (RHEA, 2014).

The UGV was equipped with a control system and four power systems: an ICE, a PV panel, a hydrogen fuel cell (HFC) and batteries. The group formed by the PV panel, the HFC and the batteries is referred as the electrical energy system (EES). Figure 1 shows the final aspect of the UGV used for the analysis and tests provided in this article. In this figure, the different subsystems whose main features are detailed in the following sections can be identified. Originally, the UGV used two alternators (12 V dc and 24 V dc), which were removed and replaced with appropriately designed and sized EES. In Section 3, the added energy system features (PV panel, hydrogen fuel cell and batteries) will be sized, justified and assessed.

2.1.1.1. UGV control system. The UGV control system (see Fig. 2) allowed an autonomous worker to apply an effective treatment with high precision. It was responsible for synchronising and processing all information selecting the best behaviour for the entire system depending on the current

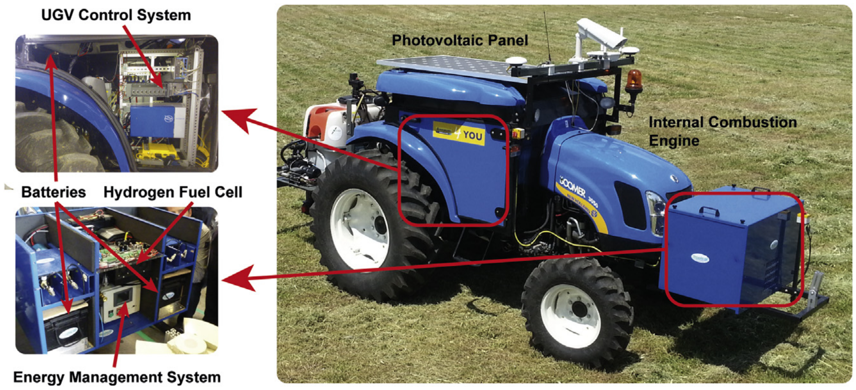

Fig. 1 – Unmanned ground vehicle (UGV).

working situation. This controller communicated with other subsystems via diverse electronic communication protocols (Ethernet, serial and CAN bus) and it interpreted the information coming from the external user and other devices (Emmi, Gonzalez-de-Soto, Pajares, Gonzalez-de-Santos, 2014a, b). The set of all of these systems (controllers, sensors and actuators) had an average power demand of approximately 170 W for 12 V dc devices and of approximately 260 W for 24 V dc devices.

The UGV was equipped with a positioning system that consisted of a GPS receiver; a Trimble Model BX982, with two antennas. This system used an RTK signal correction, provided by a base station, achieving an accuracy of approximately ±0.025 m. A second antenna was used to obtain the heading of the UGV even when the UGV was stationary (Carballido, Perez-Ruiz, Emmi, Agüera, & others, 2014).

A vision system, installed on-board the UGV, was used by the weed detection system (WDS), the row detection system (RDS) and the safety system. The RDS estimated rops rows and the WDS was able to identify weeds and crop plants even when they were contaminated with materials from the soil (Guerrero et al., 2013), (Montalvo et al., 2013).

The safety system comprised of an obstacle detection system based on a vision camera, a laser and a remote controller used by the operator. The laser on-board the vehicle was in charge of the lowest safety level and was configured to stop the vehicle motion when any type of obstacle in the UGV path was detected, considering the time to stop the vehicle (Garrido et al., 2012).

The work plan execution was supervised by a base station which generated the work plan and sent it to the UGV. When the UGV was working, this base station was responsible for monitoring the status of both the UGV and the agricultural implement in real-time and detecting failures (Conesa-Muñoz, Gonzalez-de-Soto, Gonzalez-de-Santos, & Ribeiro, 2015).

2.1.1.2. *Internal combustion engine*. The ICE could work as the only power source, providing the total power demanded by the agricultural task, or as a part of the HES, providing only the power to move the UGV with its implement. It preserved features from the original tractor, although the maximum ground speed has been limited to 7 km h^{-1} for safety reasons; thus some gears were disabled. The main ICE features are

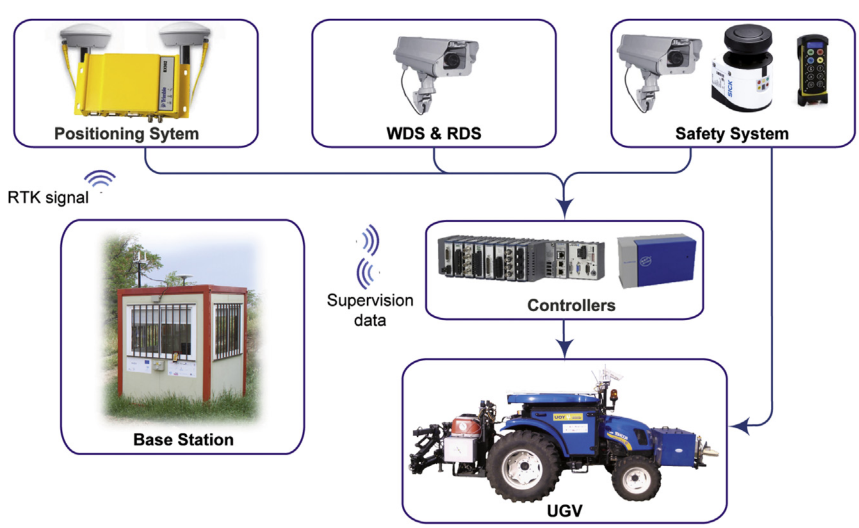

Fig. 2 – UGV control system.

Table 1 – Main features of the ICE. Source: (CNH America, 2009).

Feature	Value
Gross power	33.6 kW
Rated speed	2800 rpm
Idle speed	1050 rpm
Maximum speed	3050 rpm

compiled in Table 1. Figure 3 shows the ICE performance curves provide by the manufacturer, which were used to calculate the exhaust gas emissions and to implement the energy demand model. In this figure, torque, specific fuel consumption volume (SFC_v) and the power curve with respect to the ICE speed can be seen. These curves were used to estimate the ICE fuel consumption and the exhaust emissions.

2.1.1.3. *Hydrogen fuel cell*. An HFC was used because it provides good performance to generate electrical power (approximately 50%) and fairly rapid refuelling. It was situated in a box placed on the tractor muzzle, next to the hydrogen tanks, where there was enough space. A proton exchange membrane (PEM) fuel cell was selected and metal hydride tanks offered by the company Tropical S.A. (Athens, Greece), which has a power range from 0.5 to 5 kW with a specific hydrogen consumption (SHC) of approximately 0.74 N m^3 Kw h^{-1}. This value was used to estimate the hydrogen consumption (Tropical, 2015).

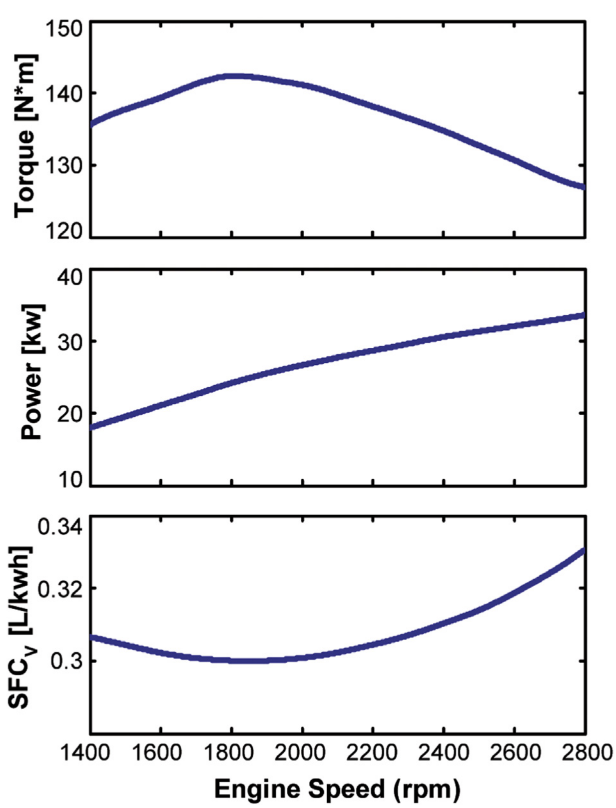

Fig. 3 – ICE performance curves. Source: (CNH America LLC, 2009).

2.1.1.4. *Photovoltaic panel*. The PV panel was used as an additional system for "free" energy, which charges the batteries whenever there is sufficient light; even when the UGV is in a garage. The panel was situated at the highest part of the UGV to minimise shadows. Only the antennas and the camera were higher to improve signal transmission and the area of view. The PV panel was set horizontally to collect solar power independently of orientation.

2.1.1.5. *Batteries*. Batteries were used to store excess electrical energy and to supply energy during high demand periods (for example during starting of the ICE) and to ensure that the vehicle's energy management system (EMS) had a continuous energy supply. Because the batteries were heavy, one group of batteries was placed over the rear axle to reduce the slippage in tasks requiring a draft force. Another battery bank was placed next to the HFC, hydrogen tanks and EMS, inside a box in the front part of the tractor and acts as counterweight, which is necessary to work with heavy implements.

2.1.1.6. *Energy management system*. The EMS was responsible for regulating and adapting the electrical power and supervising the electrical energy storage. This system consisted of a controller that managed the electrical energy flow from the HFC and PV systems. It collected data about the status of the battery and hydrogen tanks and controlled the power provided by the HFC.

2.1.2. *Fuel consumption measurement and calculation of the exhaust gas emissions*

A number of studies analysing exhaust gas emissions from ICEs have been carried out in recent years as part of the continuous interest in reducing the emissions of pollutants. Some of these works have been focused on agricultural machines. Lindgren and Hansson (2002) developed a mathematical model of a tractor and analysed the fuel consumption and engine emissions for different engine control strategies and engine transmission characteristics. Janulevičius, Juostas, and Pupinis (2013) measured the exhaust emissions and fuel composition in a real tractor during ploughing for different scenarios and correlated the results to the load factor of the tractor. These works concluded that the fuel consumption and the production of emissions depends on engine speed and load conditions. The main exhaust gas is CO_2, and its amount increases with ICE speed and the fuel consumption. The largest concentrations of CO, HC and PM are emitted when the ICE operates under a partial load and at a low speed. This contrasts to NO_x emissions which are the largest when the ICE load and speed are the highest which is when combustion temperatures are highest, improving combustion, and reducing CO, HC and PM generation.

In this work, the fuel consumption is measured using two PD400 flowmeters from Titan Enterprises Ltd. (Sherborne, Dorset, UK): One meter was installed in the fuel supply line, and the other in the return line. Fuel flow was obtained from the difference between the data measured in each flowmeter. The flowmeters had a measuring range of 1–60 L h^1. This was sufficient for the ICE used which had a maximum flow of

~30 L h^{-1}, and the rated flow of the fuel pump, which was approximately 12.54 L h^{-1}. The recommended temperature range was from 0 to 60 °C, which was slightly low for the return line requiring a small radiator to cool the returned fuel. The flowmeter accuracy was approximately ±2.5% with a low loss of pressure of 10 kPa (Titan, 2014). This fuel consumption measurement system was calibrated and validated by measuring the total mass of fuel consumed during different tests.

The exhaust gas emissions from the ICE were calculated considering the partial load and speed (work regime) of the ICE according to the ISO 8178 standard (ISO, 1996) and the fuel features specified in España (2006). To calculate the partial load, the values of wheel slippage were measured (the difference between the ground speed provided by GPS and the wheel speed provided by the control system), PTO speed, ICE speed, three-point hitch (TPH) position and terrain slope (obtained from the orthometric height in each point). Using this data and the equations of ASABE Standards, (ASAE, 2011), (ANSI/ASAE, 1995), (ASAE, 2004), (ASAE, 2003) the partial load of the ICE was calculated. With this partial load, the work regime of the ICE was obtained by interpolating the power curves of the ICE as shown in Fig. 3. With this data and the standard ISO 8178 the corresponding emission factor for each exhaust substance was estimated. The ISO standard defined the emissions factors of exhaust gasses for agricultural ICEs in eight individual work regimes, considering the maximum power and the manufacturing year of the ICE. For small ICEs, as in this case, the emission factors of NO_x and HC were joined, therefore the ISO standard defined the emission factors to calculate: CO, PM and NO_x + HC. Finally, the CO_2 emission was calculated using the chemical equation of combustion reaction (considering the other exhaust emission gasses calculated with the emission factor of the ISO standard) and the measured fuel consumption.

2.1.3. *Implements and tasks*

Three different agricultural tasks with their respective implements were considered: weed control using a flaming and a row crop cultivator implement, weed control with an herbicide patch sprayer, and pest control with a canopy sprayer. Figure 4 illustrates these three implements working in experimental fields and in the next sections the main features of each implement and their main requirements are described. Furthermore, the changes in the implements to use adequately the HES are described.

2.1.3.1. *Weed treatment with a flaming and row crop cultivator implement*. This task performed ploughing and thermal treatment using a particular mechanical-thermal machine. The WDS detected weed patches by processing the images from the camera in real time. The UGV was programmed to follow a predefined path, which fixes the initial and final point of each track (path followed by the vehicle through the treated crop). These were approximate points, and were corrected by the RDS. The area analysed in each image was a rectangle with a width of 3 m (4 rows) and length of 2 m. It was georeferenced with an accuracy of approximately 0.08 m and divided into square cells with 0.25-m sides (Emmi et al., 2014b).

The implement consists of a flaming and row crop cultivator. It performed mechanical treatment in the furrows (space between crop rows), as performed by a row crop cultivator, and a thermal in-row treatment for weed control. This flaming and row crop cultivator implement (see Fig. 4b) was used for crops with wide row spaces (approximately 750 mm) that can withstand high temperatures over short periods of times, such as maize, garlic, leek, and onion. It was controlled from the UGV, which was able to regulate the gas pressure of each burner separately in three stages: zero (off), low and high. Table 2 shows the basic features of this implement (Gonzalezde-Santos, Ribeiro, Fernadez-Quintanilla, Dorado, 2014).

Originally, this implement had two hydraulic cylinders to extend and retract the main bar, which was extended for working and retracted for transporting. These cylinders could be replaced by linear actuators with electrical motors (LINAK LA36, Guderup, Nordborg, Denmark), reducing the power demanded from the ICE and increasing the power demanded from the EES by a small amount because the main energy demand of this task was in the ploughing, which was supplied by the ICE. This implement used fuel gas for the burners, but we did not consider this fuel in the energy analysis, only the electrical power used to light these burner. This gas can be any type of biogas, whose combustion emissions are considered null.

2.1.3.2. *Weed treatment with a herbicide patch sprayer*. This task consists of the spraying of herbicides over the weed patches of herbaceous crops, such as wheat and barley. The WDS was an external system that took images using aerial robots and provides a weed map of the crop with a 272 cell size of 0.5 m. The path plan followed by the UGV was improved by applying a path planning calculation method, such as, for example, the method described in (Gonzalez-de-Soto, Emmi, Garcia, & Gonzalez-de-Santos, 2015), which obtained an important reduction in work time. This path plan fixed the point where selected nozzles were opened or closed, as well as the initial and final point of each track.

The implement used was a patch sprayer (see Fig. 4b) which was used to apply herbicide in the weed-control treatments. This implement is used for herbaceous crops, such as wheat or barley, with small row spaces (approximately 100–170 mm), and was able to activate each nozzle separately and regulate the total flow of the product applied. It had two electrical lineal actuators to extend and retract the spraying booms that are controlled by the main control system from the UGV. Table 2 presents the main features of this implement (Carballido, Perez-Ruiz, Gliever, & Agüera, 2012).

Originally, this implement used a main pump that worked with the PTO using the ICE power. The pump worked to rated power whenever a valve was open, it used a bypass line to return the product overflow, and therefore it wasted a large amounts of energy. To improve this system, this main pump was replaced by a series of small pumps, using one pump for each nozzle. The selected pump for this application was the model MG100 Micropump, (TCS Micropumps Ltd, Faversham, Kent, UK) which was able to

Fig. 4 – Implements working: (a) Flaming and row cultivator, (b) Patch sprayer, and (c) Canopy sprayer.

regulate the flow to provide sufficient flow and pressure. Furthermore, this implement control system was able to regulate the main flow (the sum of each nozzle flow) to ensure and improve the correct operation. This change generated an significant reduction of the power demanded from the ICE and slightly increased the power demanded from the EES.

2.1.3.3. *Pest control with a canopy sprayer*. This task consists of spraying insecticides into tree canopies for pest control. The path plan only fixed the initial and final point of each track, and the UGV was responsible for designing the path to follow. The implement was an autonomous canopy sprayer (see Fig. 4c) that sprayed a pesticide solution over the tree canopies and blew the spray along the entire canopy. The

Table 2 – Main features of the implements. Source: (RHEA, 2014), (LINAK, 2015), (TCS, 2015.), (EBM-PAPST, 2015).

Implement	Feature	Value
Flaming and row crop cultivator	Power of implement controller	40 W (24 V)
	Number of burners (2 per row)	8
	Power of valves and sensors	<1 W
	Power of each ignitor	144 W (24 V)
	Linear actuator motor power (x2)	240 W (24 V)
Patch sprayer	Power of implement controller	40 W (24 V)
	Number of nozzles	12
	Nozzle nominal flow	0.757 L min^{-1}
	Nozzle nominal pressure	276 kPa
	Power of each pump	16.5 W (24 V)
	Power of flow control system	15 W (12 V)
	Motor power of each linear actuator (x2)	200 W (12 V)
Canopy sprayer	Power of implement controller	40 W (24 V)
	Number of diffusors	8
	Nozzle nominal flow (2 per diffusor)	0.4 L min^{-1}
	Nozzle nominal pressure	300 kPa
	Power of each pump	19 W (24 V)
	Power of flow control system	24 W (24 V)
	Air flow per nozzle	~30 m^3 min^{-1}
	Power of each fan	105 W (24 V)
	Ultrasonic sensors power	12 W (24 V)
	Motor power of each angle regulator (x4)	36 W (24 V)

redesigned canopy sprayer was designed to spray trees planted in rows spaced at approximately 4 m apart, for example in olive groves. The implement was autonomous and the main control system on the UGV only turned the implement on and off. It has eight diffusors separated by 0.6 m, four of which (the lower and upper) adapted the spray direction to the canopy from -15° to 15° with respect to its initial position. Each of these diffusors was equipped with two nozzles and one air outlet, and the implement control system was able to activate each diffusor separately. It used eight ultrasonic sensors to detect the tree canopy to activate the adequate diffusors and regulate the diffusors positions, and it is able to regulate the main flow of insecticide and air. Table 2 shows the main features of this implement (Sarri, Lisci, Rimediotti, & Vieri, 2014).

Similar to the patch sprayer, this canopy sprayer originally used the ICE power from the PTO to operate the main pump and the fan to disperse the pest control product throughout the tree canopy. In this study the implement was autonomous and the UGV main control did not know the instantaneous power requirements of the task. Thus, the pump and the fan worked at the rated power continuosly, wasting large amounts of energy. The system could be improved using a similar process to the previous case: replacing the main pump by a series of small pumps and the main fan by some small fans, using one pump and one fan in each diffusor. For this task, there were very similar requirements and therefore can the same pump model, MG100 Micro Pump could be used, and the axial compact fan EC W1G250-HH37-52 (ebm-papst Group, Mulfingen, Baden-Württemberg, Germany) was able to provide sufficient air flow. In this implement the main control was of product flow and air flow control was not necessary. The reduction of power demand from the ICE was the largest of the three cases, and the power demanded from the EES was also the largest.

2.2. *Energy demand model*

To estimate the total energy consumed in each agriculture task, the instantaneous power, the time and the relationship with the energy source were all required. The UGV had four energy sources: fuel, hydrogen, batteries and solar power although the instantaneous power provided by the sun cannot be regulated. In the energy demand model, two values were obtained: (a) the energy demand supplied by the ICE, the energy used to move the UGV and the implement, and (b) the electrical energy demand supplied by the EES. The total energy (TE) consumed could be calculated using

$$TE = E_{ESS} + E_{ICE}. \tag{1}$$

where E_{EES} is the energy supplied by the ESS and E_{ICE} the energy supplied by the ICE. To design and size the EES, the energy supplied by these systems can be calculated by

$$E_{EES} = \int_t P_{ESS}(t) = \int_t P_{UGV\ control}(t) + P_{IMP\ control}(t) + P_{Task}(t) \tag{2}$$

where P_{EES} is the instantaneous power demanded to the EES; $P_{UGV\ control}$ is the power used to supply the UGV control system described in the Section 2.1.1; $P_{IMP\ control}$ is the power consumed by the electrical control system of the implement: controllers, sensors, position actuator, etc.; and P_{Task} is the electrical power used to apply the treatment, whose values are defined

$$P_{Task} = nP_{Tool} \tag{3}$$

where n is number of tools active and P_{Tool} is the electrical power consumed by each tool. A tool is defined as a set of systems that can be activated separately to correctly apply the treatment in a given zone. With the flaming and row cultivator implement, a tool is the set of two burners and hoes used in each crop row, which use two ignitors (only to start) and two valves (only to change the status); in the patch sprayer, a tool is each nozzle, which used a pump; and in the canopy sprayer, a tool is the set of two nozzles and an air outlet of each diffusor, which use a pump and a fan.

Furthermore, we can estimate the energy provides by the ICE as

$$E_{ICE} = \int_t P_{ICE}(t) = \int_t [D(t) + MR(t)]v(t) \tag{4}$$

where v is the system speed (m s^{-1}); D is the implement draft force (kN), which depends on the dimensionless soil texture adjustment parameter and the machine-specific parameters; MR is the motion resistance (kN), which depends of the soil surfaces, terrain slope, wheel slip, total system mass and UGV tyres. This expression calculated the energy obtained from the ICE, it did not take into account the losses of mechanical and traction efficiency in the UGV (ASAE, 2011), (ANSI/ASAE, 1995), (ASAE, 2004), (ASAE, 2003).

3. Case studies

In this section, the energy requirements of each task are studied and the design process followed is analysed. The results obtained using this HES to perform the treatments to crops are described.

3.1. *Energetic analysis*

The energy requirements of each studied task were analysed using the energy model previously descrfibed. Using these data, the necessary features of the HES are presented and the real devices used in the HES are defined.

3.1.1. *Energy demand*

In this section, the electrical energy requirements supplied by the EES for the three agriculture tasks studied are analysed: pest control using insecticides, weed control using ploughing and flaming and weed control using herbicide. To carry out this energy estimation, a representation of real crops was used (see Fig. 5) where the experimental tests that are analysed in Section 3.2 are used. The model described in Section 2.2 was used to estimate the total energy consumed as maximum power demand and average power. Also, this power was split into two values: the power demanded by the 24-V dc systems and the one demanded by the 12-V dc systems.

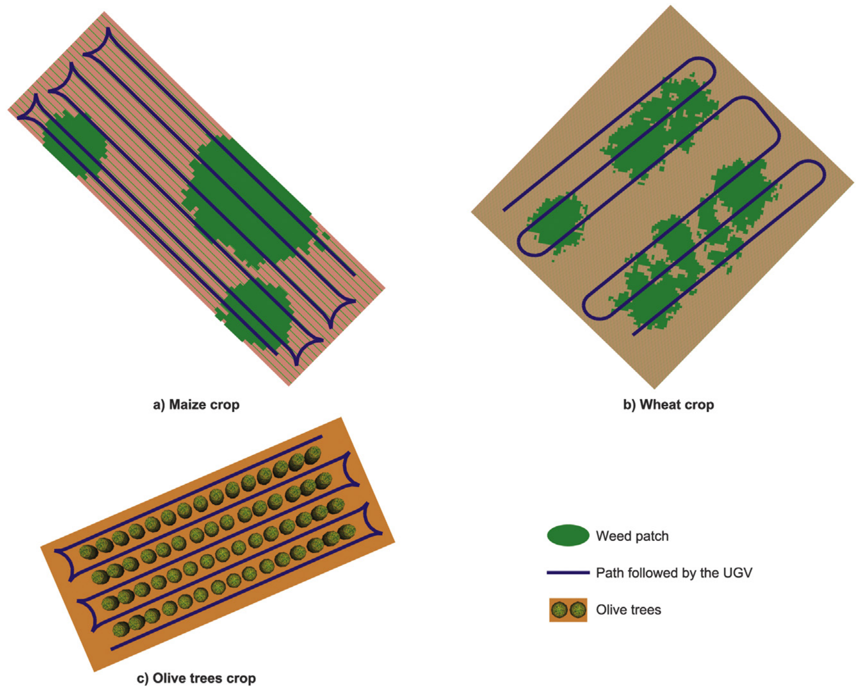

Fig. 5 – Test bench.

3.1.1.1. *Energy analysis in weed control using the flaming and row crop cultivator implement*. Figure 6 represents the electrical power demand of the 12-V dc devices, 24-V dc devices and the sum of both. For this task, it was observed that the demand from the 12-V dc devices was almost constant and that the demand of 24-V dc system had abrupt and very short peaks, which were generated by the burner ignitors. Table 3 presents the values of these peaks, and the average values of each represented power demand. The total hydrogen consumed during a working shift of 8 h was calculated, assuming that the HFC, described in Section 2.1.1, supplied all of the electrical energy. This task represented the lowest power demand from the EES because ploughing was supplied by the ICE, and the gas does not need power to work, only an ignition spark; thus, the EES is basically used to power the electrical control systems.

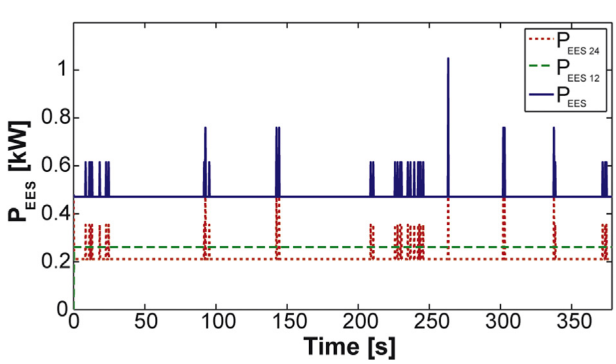

Fig. 6 – Power demands in weed control using the flaming and row crop cultivator implement.

3.1.1.2. *Energy analysis in weed control using the patch sprayer*. Figure 7 illustrates the instantaneous power demand in the weed control task applying herbicides using the UGV with the patch sprayer. In this case, it can be observed that the power used by the 12-V dc systems was almost constant because they were mainly control systems but the power demanded by the 24-V dc systems had important variations that occurred when the pumps applied the treatment to weed patches. Table 3 presents the maximum values of the power demand, their average values and the total hydrogen consumed during a working day of 8 h. Values that, in general, increase with respect to the above cases.

3.1.1.3. *Energy analysis in pest control tasks using the canopy sprayer*. As in the other tasks, Fig. 8 shows the power demanded in pest control using the autonomous canopy

Table 3 – Power and hydrogen consumed in each application.

	Implement		
	Flaming and row crop cultivator	Patch sprayer	Canopy sprayer
12 V average power	0.26 kW	0.28 kW	0.26 kW
24 V average power	0.22 kW	0.28 kW	0.90 kW
Total average power	0.48 kW	0.56 kW	1.16 kW
12 V maximum power	0.26 kW	0.40 kW	0.26 kW
24 V maximum power	0.79 kW	0.41 kW	1.39 kW
Total maximum power	1.05 kW	0.68 kW	1.65 kW
H_2 consumed (for 8 h)	2.43 Nm^3	2.84 Nm^3	5.96 Nm^3

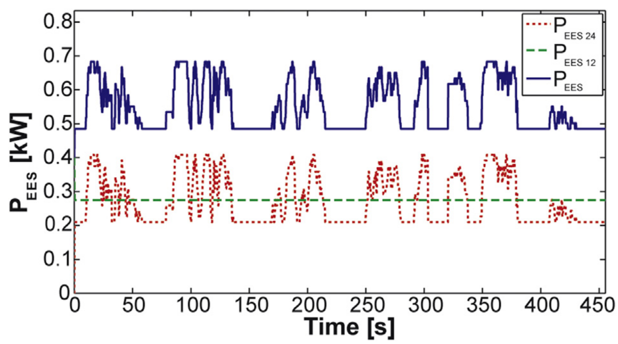

Fig. 7 – Power demands in weed control using the sprayer implement.

sprayer. These graphs are quite similar to the last analysed case, but with larger values in the power demanded of the 24-V systems, the only voltage used in this implement. These numerical values can be seen in Table 3 and compared to the above cases. As expected, this task had the highest power demand from the EES although the power demand from the 12-V dc systems was quite similar to the other three cases because it was used mainly by the control systems. Thus, the controllers had a quasi-constant power demand, and were not strongly influenced by the task performed.

3.1.2. *Hybrid energy system*

The energy system studied here used the original ICE of the tractor operating in parallel with the EES. Figure 9 presents the architecture of the HES. It can be seen that the ICE was used to provide motion, overcoming the MR and the possible draft forces generated by the implement, and the EES was used to power all electrical systems of the UGV. The ICE had enough power and autonomy for the task analysed in this work, but an EES needed to be designed to supply the electrical energy requirements of each agricultural task.

The EES used hydrogen as the main energy source with a small contribution from PV energy. It used batteries to adapt the power to the energy requirement and store the electric energy generated by the PV panel when it was not in use. The EES was designed according the maximum values in Table 3.

The hydrogen system was designed to supply the average power demanded by all electric system, control systems, sensors, actuators, etc. Therefore, an HFC with a minimum power of 1.16 kW and a hydrogen storage of at least 5.96 Nm^3 was required. The HFC used was based on TROPICAL TB-1000 model. It is an unregulated DC power system based on PEM fuel cell technology (FCgen-1020ACS, Ballard Power Systems, Burnaby, British Columbia, Canada). It has to be fuelled with pure hydrogen and is able to deliver up to 1.4 kW peak electrical power and 1.2 kW in nominal continuous power operation. Metal hydride tanks were used as a hydrogen storage system, and a minimum of 2 tanks with capacities of 3 Nm^3 was required. However, for further The PV panel used was a Module EGM-185 (EGing PV Co., Ltd, Jintan, Jiangsu, P.R.C), which had a power rating of 183 W with an efficiency of approximately 15%. In the test bench location (40°18′29″ N, 3°29′14″ W), this panel provided an average energy per day of 0.88 kWh, with a maximum of 1.46 kW h day^{-1} in July according the irradiation data available from the PV Geographical Information System of the Institute for Energy and Transport (PVGIS, 2015).

With respect to the batteries, deep-cycle lead-acid batteries were used which can be discharged using most of their capacity and supply current demands greater than the current provided by in the short term by the HFC. They were charged by both the HFC and PV panel and stored all unused PV energy. The batteries were divided into two banks: one bank to supply the 12-V dc systems and the other bank for the 24-V dc systems. Each group was formed by two batteries with 2.2 kW h of capacity; this capacity is enough to store the PV energy over several days of inactivity and sufficient to satisfy at sporadic instantaneous high energy demands, such as the ones shown in Fig. 8. Table 3 shows that the power demands of the 24-V dc systems are higher, but this does not consider the energy required to start the ICE. Furthermore, because deep-cycle batteries were used, two or more batteries in parallel were required to start the ICE.

The EMS is responsible for (a) regulating and adapting the power provided by the HFC and the PV panel; (b) assuring a minimum charge in the batteries; (c) obtaining the maximum PV power; and (d) supervising hydrogen storage, batteries status and PV power. It used two solar controllers with maximum power point tracking (MPPT SS-MPPT-15L, Morningstar, Inc., Chicago, Illinois, US) to obtain the maximum power from the PV panel: one for the 12-V batteries and another one for 24-V batteries. Two DC battery chargers (BCD1015, Analytic Systems Ware Ltd, Delta, British Columbia, Canada), were required to adapt the power from the HFC. Two chargers were required for each battery voltage. The EMS was equipped with a controller that managed the energy flow. The block diagram of the EMS is shown in Fig. 10, where C_{12V}, C_{24V} are the charges of the 12- and 24-V batteries, respectively; C12V min and C24V min are the minimum charge in these batteries with the HFC stopped and $C_{12V\ MAX}$ and $C_{24V\ MAX}$ are the maximum charges in these batteries with the HFC running. The values C12V min and C24V min are calculated to ensure correct operation during high energy demand periods. The $C_{12V\ MAX}$ and $C_{24V\ MAX}$ values were calculated to create a hysteresis cycle for the HFC operation with a value that is high enough to avoid excessive start/stop on the HFC but low enough to allow for the storage of the PV energy generated when the UGV was stationary.

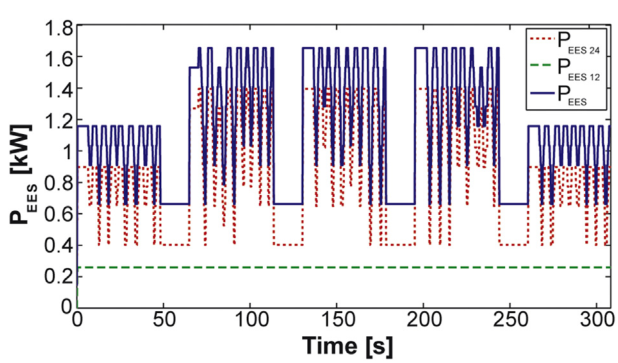

Fig. 8 – Power demand in pest control tasks using the canopy sprayer implement.

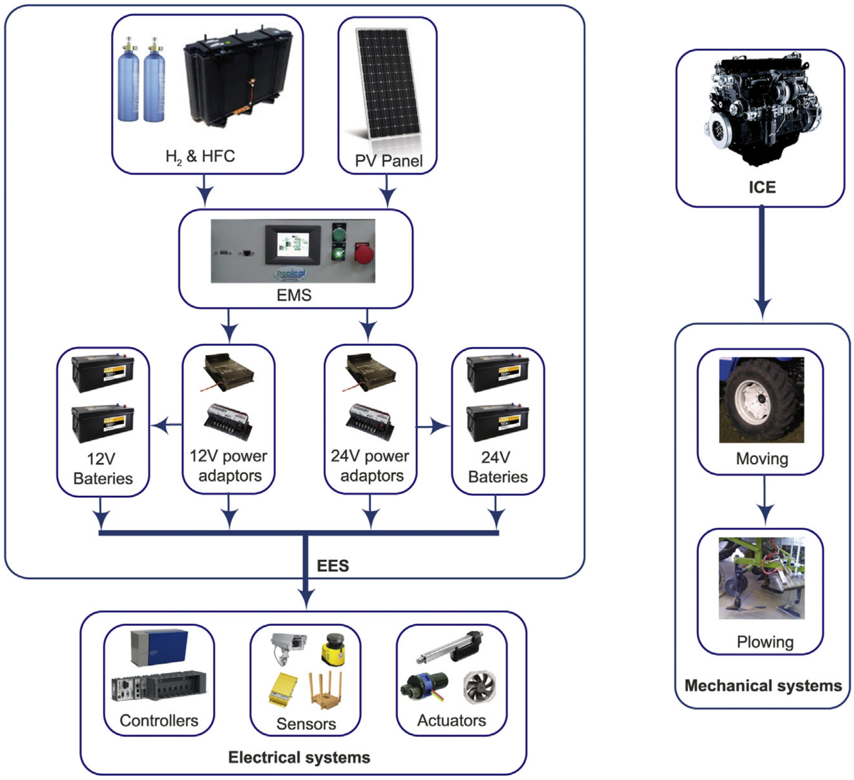

Fig. 9 – Hybrid energy system.

3.2. *Results and discussion*

In this section, the emission reductions obtained by using the HES in the UGV under real scenarios are presented. To analyse the results, the emissions using the UGV with the ICE as the only power system were compared with the UGV using the HES described in Section 3.1.2. The same UGV was used for all tests, and fuel consumption and emissions were measured as explained in Section 2.1.2. The experimental test benches were the crops represented in Fig. 5.

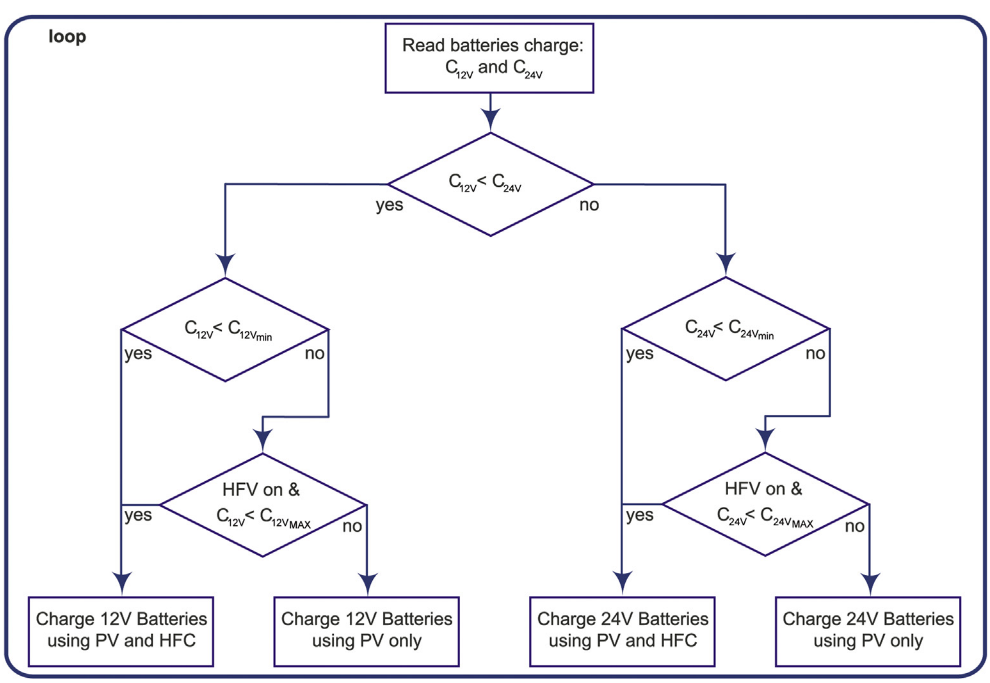

Fig. 10 – Block diagram of the flow energy control.

3.2.1. *Hybrid power in weed control for fire resistant crops with wide furrows: ploughing and flame weed treatment*

This test is performed over the maize crop shown in Fig. 5a, where the path followed by the UGV and the weed patch treated can be seen. As described in Section 2.1.3.1, the UGV detected the weed patches in real time, therefore, path planning covered the entire field. Although the burners were only activated over weeds patches, the hoes ploughed all furrows to control weeds and aerate the soil. Therefore, there was an important energy demand required to plough all tracks and exhaust gas flow increased, especially the CO_2, as can be see in Fig. 11a, which shows the exhaust gas flow emitted with respect to UGV position. This required energy to plough was the main demand and it was supplied by the ICE in both cases (i.e. using the ICE alone and using it with the HES). Therefore, the emission reduction obtained due by using the HES was low. As can be seen in Fig. 11 and in Table 4, the reduction of air pollution during this task was low, much lower than in the other analysed tasks, as will be seen in the next sections. The CO_2 emission showed only a small reduction due to the energy consumed by the ignitors of the flamers and the electric control system, although the energy consumed by the ignitors was almost negligible.

3.2.2. *Hybrid power in weed control on herbaceous crops: spraying of herbicides*

This test was performed over the wheat crop shown in Fig. 5b. From the weed map the path followed by the UGV to treat all weed patches can be seen. The weed map was known in advance of the treatment and therefore the path could be optimised to obtain energy reductions. In this case, the method described by (Gonzalez-de-Soto et al., 2015) was used to calculate the path. In Fig. 5b, all tracks had the same weed zone so that the track path direction was adapted to the shape of the weed patches.

Table 4 – Average values and comparison of exhaust gas emissions in weed control using the flaming and row crop cultivator implement.

	Units	CO_2	CO	$HC + NO_X$	PM
System with only ICE	$g\,h^{-1}$	11,320	113.2	147.8	12.6
	$g\,kWh^{-1}$	561	5.61	7.32	0.63
Hybrid system	$g\,h^{-1}$	10,355	112.9	147.5	12.6
	$g\,kWh^{-1}$	514	5.61	7.32	0.63
Exhaust gas reduction[a]	%	8.53	0.2	0.2	0.0

[a] With respect to the emissions per hour.

Figure 12 shows the instantaneous emissions of CO_2, CO, $HC + NO_X$ and PM, and Table 5 shows their average values and the reductions obtained when using the HES. Figure 12a shows a significant reduction in CO_2 because the HES avoids the use of the PTO, resulting in a significant reduction in fuel consumption. Figure 12c presents the reduction of the emissions of HC and NO_X, but they are lower than the reduction in CO_2. This occurs because the NO_X concentration in the exhaust gasses decreases with the ICE speed but the concentration of HC increases. PM emissions were very similar in both cases (see Fig. 12d) because PM concentrations in exhaust gases increase as ICE speed decreases, as was the case here when the PTO was off or operating slowly. A similar result occurred with the CO, but to a lesser extent, as can be seen in Fig. 12b

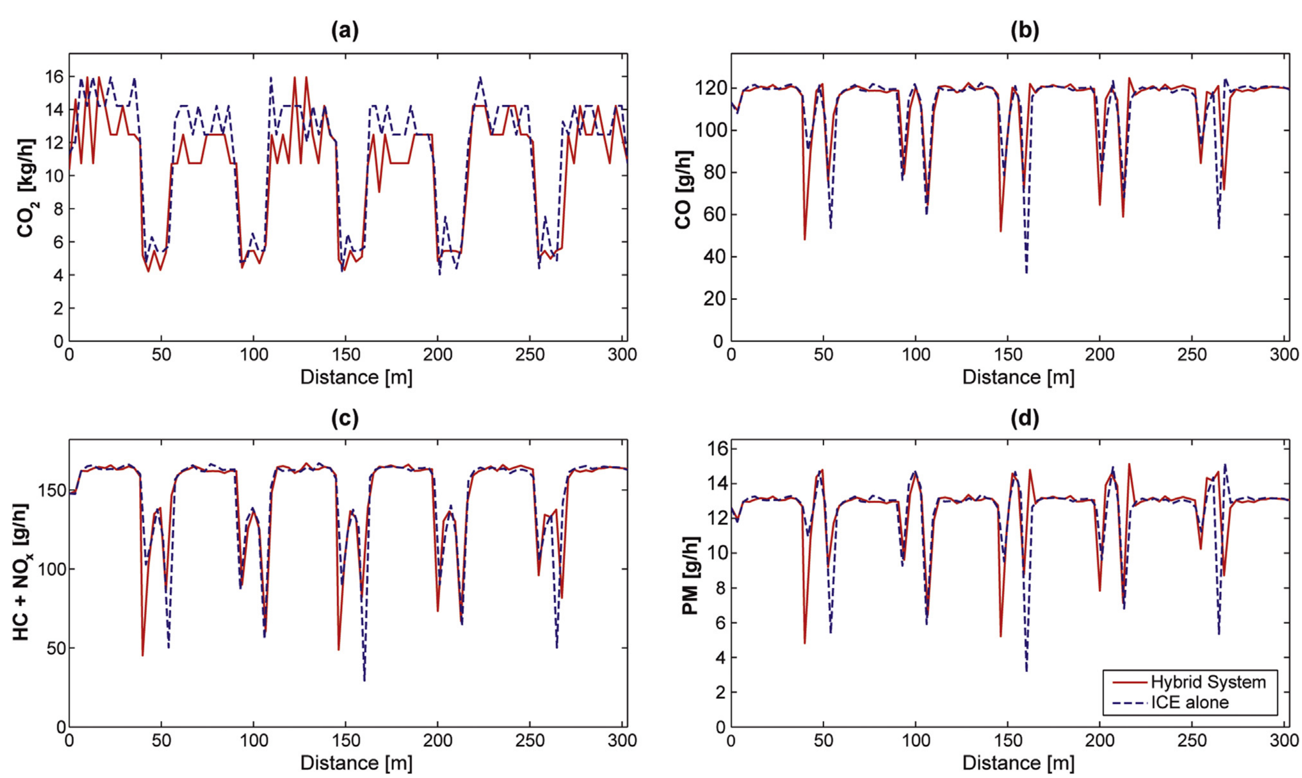

Fig. 11 – Exhaust gas emissions in weed control using the flaming and row crop cultivator implement.

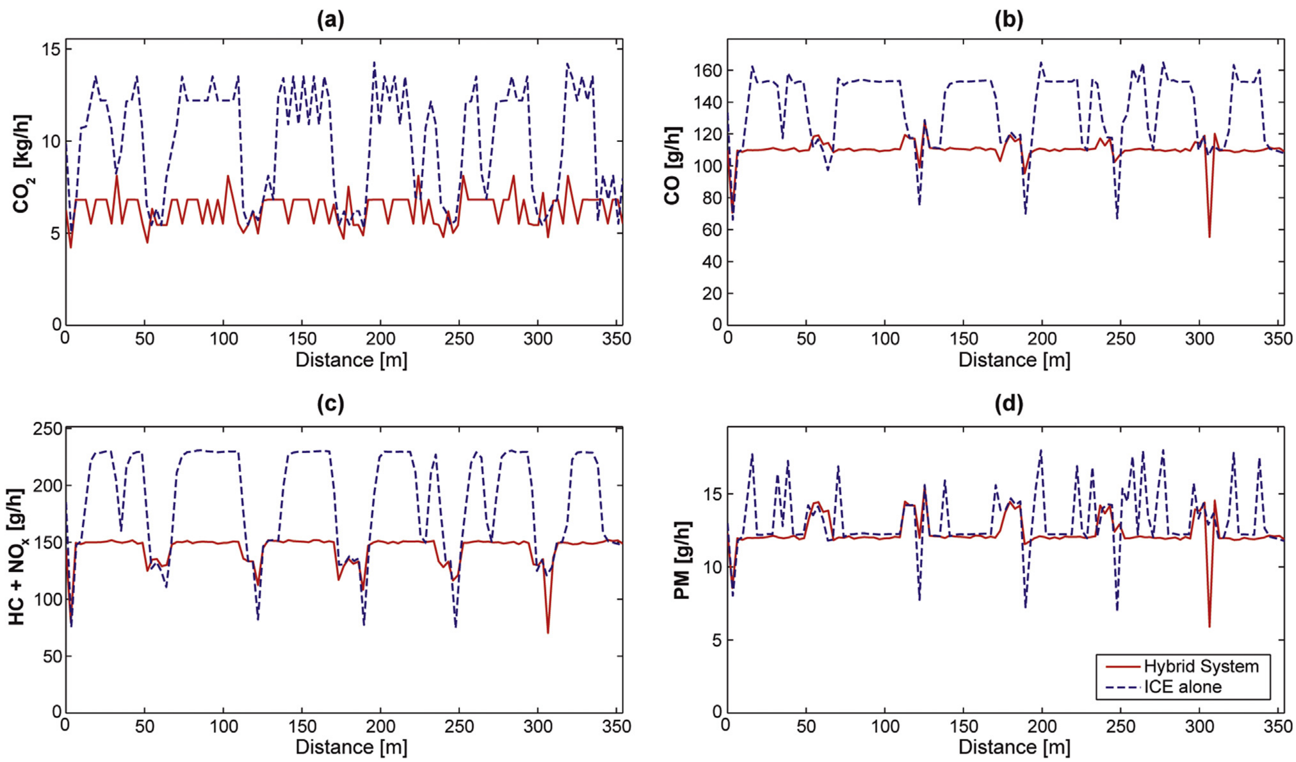

Fig. 12 – Exhaust gas emissions in weed control using the patch sprayer.

and in Table 5. It can be observed that the CO and PM emissions respect to the energy (g kW h^{-1}) increased when the HES was used due to the effect of decreasing ICE speed. In numerous works that analysed ICE exhaust gases, similar emission results have been obtained for these gases (Janulevičius et al., 2013; Lindgren & Hansson, 2002; Lindgren et al., 2011; Li, McLaughlin, Patterson, Burtt, & others, 2006; and Labeckas and Slavinskas, 2013).

3.2.3. *Hybrid power for the pest control on trees: fumigation using insecticides*

These tests were performed in the small olive grove shown in Fig. 5c, where the path followed by the UGV can be seen. As described in Section 2.1.3.3, the implement used for this task was an autonomous canopy sprayer, which detected and sprayed all trees along the track. The path must therefore pass along both sides of each tree in the crop.

Table 5 – Average values and comparison of the exhaust gas emissions in the weed control using the patch sprayer.

	Units	CO_2	CO	HC + NO_X	PM
System with only ICE	g h^{-1}	9860	133.4	185.2	13.0
	g kWh^{-1}	390	5.28	7.33	0.62
Hybrid System	g h^{-1}	6253	109.7	143.4	13.0
	g kWh^{-1}	317	5.57	7.29	0.51
Exhaust gas reduction[a]	%	36.6	17.8	22.6	5.4

[a] With respect to the emissions per hour.

As shown in Section 3.1.1, this implement demands the most energy from the EES of the three analysed implements and therefore the highest power demand reduction from the ICE was achieved. This reduction is shown in Fig. 13 and Table 6, where the highest reduction in the exhaust gases out of the three analysed tasks can be observed. The reduction in CO_2 emissions almost reached 50%. The results are quite similar to the previous case (herbicide spraying) but with greater reduction in emissions, except for PM emissions, which presents a lower emission reduction with canopy sprayer. This is because in this case, when the ICE supplied all of the energy requirements, its PM emissions were the lowest out of the three cases analysed. This occurred because the PTO operated at its rated power during the entire operation and the PM concentration in the ICE exhaust gases was at its lowest. In Table 6 it can be observed that CO and PM emissions with respect to energy (g kW h^{-1}) are again lower when the ICE is used alone since with the HES the ICE works at low speed. Although the concentration of CO and PM in the exhaust gases was the lowest for this ICE speed and load, the total of exhaust gases increased such that, using the ICE alone, the emissions (g h^{-1}) of CO and PM were greater than using the HES.

4. Conclusions

This work demonstrates that it is possible to combine current agricultural machines, which use ICEs for power, with new technologies that are based on clean energy sources to obtain significant reductions in the emission of atmospheric

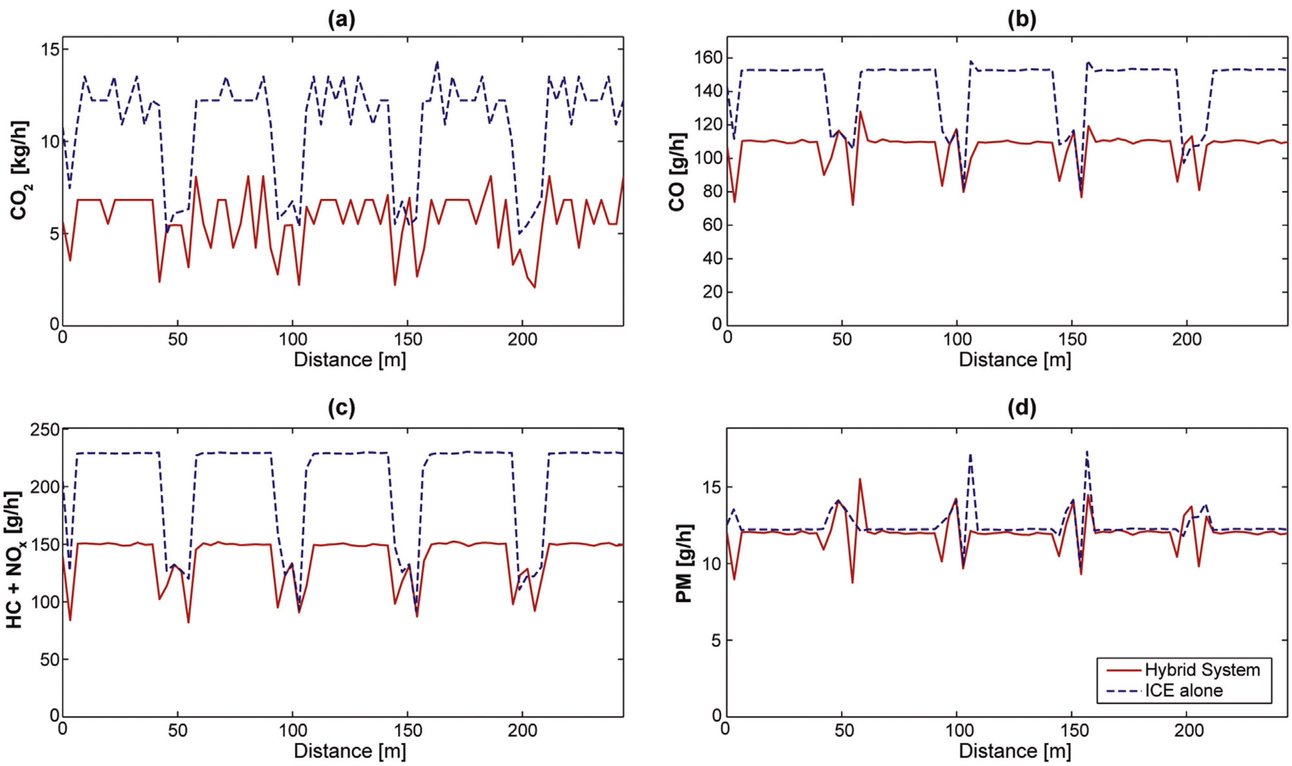

Fig. 13 – Exhaust gas emissions in pest control tasks using the canopy sprayer.

pollutants and greenhouse gases. This occurred by offloading the ICE and adding this load to an additional EES. This approach allows for the use of small agricultural tractors to move larger implements that have their own motors by the addition of an EES. This is especially interesting for agricultural tasks because, normally, the size and height are usually not problems for tractors. Furthermore, it is sometimes necessary to add weight to agricultural tractors to help reduce slippage or act as a counterweight. Agricultural tasks with draft force often require additional weight to reduce slippage. When draft force is negligible, but a heavy implement is used to apply a product, counterweights are required.

The technique of adding an EES appears very effective for tasks where the implement requires PTO power, as shown in Sections 3.2.2 and 3.2.3. The replacement of this PTO power is relatively simple; only small changes were required in the implement, as those described in Section 2.1.3. When the implement generated draft force, such as in ploughing, this technique was not as effective as in the case analysed in Section 3.2.1, but a reduction in the pollutant emissions was obtained from these robotic systems when the electric energy consumption was important.

The use of EES allows small electrical actuators to be used, which are able to apply the treatments in small areas consuming very little power. This use of distributed systems is especially interesting in precision agriculture, where the treatment is focused on the affected area, which is often smaller than the total area that the implement is able to treat. As found here, the use of a main motive power system can waste energy to carry out the same treatment. Furthermore, the losses from electrical energy transport are lower than the losses due to friction in mechanical energy transmission systems.

The greatest improvement is the results was obtained by the autonomous implement analysed in Section 3.2.3. In this case, the UGV did not know the instantaneous power requirements of the implement, and thus, for the case in which the ICE is the only power source, the ICE must supply the rated power to the implement, which is a very inefficient use of energy. However, with the HES, the implement uses the energy provided by the EES, and it is able to manage its energy, using only the required amount.

The theoretical studies and experiments conducted in this work reveal that the use of a HES in precision agriculture using robotic tractors improves the quality of the exhaust gasses and the energy use. Robotic tractors have increased electricity consumption compared to traditional tractors; therefore, it is very interesting to add an EES when the tractor is robotised

Table 6 – Average values and comparison of the exhaust gas emissions in pest control tasks using the canopy sprayer implement.

	Units	CO_2	CO	$HC + NO_X$	PM
System with only ICE	$g\ h^{-1}$	10,739	142.5	204.7	12.5
	$g\ kWh^{-1}$	378	5.01	7.19	0.44
Hybrid System	$g\ h^{-1}$	5640	107.1	139.3	12.0
	$g\ kWh^{-1}$	286	5.43	7.06	0.61
Exhaust gas reduction[a]	%	47.5	24.8	32.0	3.8

[a] With respect to the emissions per hour.

because the use of alternators increases the energy losses. Furthermore, an EES can be designed to supply some of the energy requirements of the agricultural task, as in this work. The HES achieved a significant reduction in atmospheric pollutant emissions, such as CO_2, CO, NO_X, HC and PM, which can cause environmental changes and health issues. This work has demonstrated that, currently, the use of this type of HES provides reliability and autonomy and that it can be used in all agricultural tasks with any tractor, offloading the ICE to a greater or lesser extent, which can be regarded as an intermediate step towards the use of completely clean energy systems.

Acknowledgements

The research leading to these results received funding from the European Union's Seventh Framework Programme [FP7/2007-2013] under Grant Agreement nº 245986.

REFERENCES

ANSI/ASAE. (1995). *S296.4 DEC95 Agricultural machinery management data* (pp. 118–120). St. Joseph, MI, USA: ASAE Standards.

ASAE. (2003). *D497.4 FEB2003 Agricultural machinery management data* (pp. 273–280). St. Joseph, MI, USA: ASAE Standards.

ASAE. (2011). *D497.7 MAR2011 Agricultural machinery management data* (pp. 372–380). St. Joseph, MI, USA: ASAE Standards.

ASAE. (2004). *S313.3 FEB04 Soil cone penetrometer* (pp. 903–904). St. Joseph, MI, USA: ASAE Standards.

Carballido, J., Perez-Ruiz, M., Emmi, L., Agüera, J., &, others. (2014). Comparison of positional accuracy between RTK and RTX GNSS based on the autonomous agricultural vehicles under field conditions. *Applied Engineering in Agriculture, 30*, 361–366.

Carballido, J., Perez-Ruiz, M., Gliever, C., & Agüera, M. (2012). Design, development and lab evaluation of a weed control sprayer to be used in robotic systems. In *Proceedings of the First International Conference on Robotics and Associated High-Technologies and Equipment for Agriculture. Presented at the Applications of automated systems and robotics for crop protection in sustainable precision agriculture* (pp. 23–29). Pisa, Italy: Pisa University Press srl.

Clements, D. R., Weise, S. F., Brown, R., Stonehouse, D. P., Hume, D. J., & Swanton, C. J. (1995). Energy analysis of tillage and herbicide inputs in alternative weed management systems. *Agriculture Ecosystems & Environment, 52*, 119–128. http://dx.doi.org/10.1016/0167-8809(94)00546-Q.

CNH America LLC. (2009). *BOOMER 3040, 3045, 3050 CVT service manual complete contents*.

Conesa-Muñoz, J., Gonzalez-de-Soto, M., Gonzalez-de-Santos, P., & Ribeiro, A. (2015). Distributed multi-level supervision to effectively monitor the operations of a fleet of autonomous vehicles in agricultural tasks. *Sensors, 15*, 5402–5428. http://dx.doi.org/10.3390/s150305402.

Dalgaard, T., Halberg, N., & Porter, J. R. (2001). A model for fossil energy use in Danish agriculture used to compare organic and conventional farming. *Agriculture Ecosystems & Environment, 87*, 51–65. http://dx.doi.org/10.1016/S0167-8809(00)00297-8.

Delucchi, M. A., & Lipman, T. E. (2001). An analysis of the retail and lifecycle cost of battery-powered electric vehicles. *Transportation Research Part D: Transport and Environment, 6*, 371–404. http://dx.doi.org/10.1016/S1361-9209(00)00031-6.

Dictionary - WordReference.com [WWW Document], URL http://www.wordreference.com/(accessed 6.5.15).

Eaves, S., & Eaves, J. (2004). A cost comparison of fuel-cell and battery electric vehicles. *Journal of Power Sources, 130*, 208–212. http://dx.doi.org/10.1016/j.jpowsour.2003.12.016.

EBM-PAPST [WWW Document], World market leader for energy-saving fans and motors. URL http://www.ebmpapst.com/en/ (accessed 30.4.15).

Emmi, L., Gonzalez-de-Soto, M., Pajares, G., & Gonzalez-de-Santos, P. (2014a). New trends in robotics for agriculture: integration and assessment of a real fleet of robots. *The Scientific World Journal, 2014*, 21. http://dx.doi.org/10.1155/2014/404059.

Emmi, L., Gonzalez-de-Soto, M., Pajares, G., & Gonzalez-de-Santos, P. (2014b). Integrating sensory/actuation systems in agricultural vehicles. *Sensors, 14*, 4014–4049. http://dx.doi.org/10.3390/s140304014.

EPA, U. S. Environmental Protection Agency [WWW Document]. URL http://www.epa.gov/(accessed 4.9.15).

España. (2006). *Real Decreto 61/2006, de 31 de enero, por el que se determinan las especificaciones de gasolinas, gasóleos, fuelóleos y gases licuados del petróleo y se regula el uso de determinados biocarburantes*. Boletín Oficial del Estado, 17 de febrero de 2006, núm. 41 (pp. 6342–6357).

Garrido, M., Ribeiro, A., Barreiro, P., Debilde, B., Balmer, P., Carballido, J., et al. (2012). Safety functional requirements for robot fleets for highly effective agriculture and forestry management (RHEA). In *Proceedings of the international conference of agricultural enginerring*. Spain: CIGR-AgEng2012. Valencia. July 8-12.

Gasparatos, A., Stromberg, P., & Takeuchi, K. (2011). Biofuels, ecosystem services and human wellbeing: putting biofuels in the ecosystem services narrative. *Agriculture Ecosystems & Environment, 142*, 111–128. http://dx.doi.org/10.1016/j.agee.2011.04.020.

Gonzalez-de-Santos, P., Ribeiro, A., Fernadez-Quintanilla, C., & Dorado, J. (2014). Assessing a fleet of robots for herbicide applications. In *Proceedings International Conference of Agricultural Engineering. Presented at the International Conference of Agricultural Engineering*. Zurich, Switzerland: GEYSECO.

Gonzalez-de-Soto, M., Emmi, L., Garcia, I., & Gonzalez-de-Santos, P. (2015). Reducing fuel consumption in weed and pest control using robotic tractors. *Computers and Electronics in Agriculture, 114*, 96–113. http://dx.doi.org/10.1016/j.compag.2015.04.003.

Guerrero, J. M., Guijarro, M., Montalvo, M., Romeo, J., Emmi, L., Ribeiro, A., et al. (2013). Automatic expert system based on images for accuracy crop row detection in maize fields. *Expert Systems with Applications, 40*, 656–664. http://dx.doi.org/10.1016/j.eswa.2012.07.073.

Guzmán, G. I., & Alonso, A. M. (2008). A comparison of energy use in conventional and organic olive oil production in Spain. *Agricultural Systems, 98*, 167–176. http://dx.doi.org/10.1016/j.agsy.2008.06.004.

Hansson, P.-A., Lindgren, M., & Norén, O. (2001). PM – power and machinery: a comparison between different methods of calculating average engine emissions for agricultural tractors. *Journal of Agricultural Engineering Research, 80*, 37–43. http://dx.doi.org/10.1006/jaer.2001.0710.

ISO. (1996). *8178-4:1996–Reciprocating internal combustion engines – exhaust emission measurement – Part 4: test cycles for different engine applications* (International Organisation of Standardisation).

Januleviičius, A., Juostas, A., & Pupinis, G. (2013). Tractor's engine performance and emission characteristics in the process of ploughing. *Energy Conversion and Management, 75*, 498–508. http://dx.doi.org/10.1016/j.enconman.2013.06.052.

Labeckas, G., & Slavinskas, S. (2013). Performance and emission characteristics of a direct injection diesel engine operating on KDV synthetic diesel fuel. *Energy Conversion and Management, 66*, 173–188. http://dx.doi.org/10.1016/j.enconman.2012.10.004.

Li, Y. X., McLaughlin, N. B., Patterson, B. S., Burtt, S. D., & others. (2006). Fuel efficiency and exhaust emissions for biodiesel blends in an agricultural tractor. *Canadian Biosystems Engineering/Le Genie des biosystems au Canada, 48*, 2.

LINAK [WWW Document], n.d.. Tecnológica Actuadores Lineales LINAK Actuadores SLuSpain Port. URL http://www.linak.es/ (accessed 28.4.15).

Lindgren, M., Arrhenius, K., Larsson, G., Bäfver, L., Arvidsson, H., Wetterberg, C., et al. (2011). Analysis of unregulated emissions from an off-road diesel engine during realistic work operations. *Atmospheric Environment, 45*, 5394–5398. http://dx.doi.org/10.1016/j.atmosenv.2011.06.046.

Lindgren, M., & Hansson, P.-A. (2002). PM – power and machinery: effects of engine control strategies and transmission characteristics on the exhaust gas emissions from an agricultural tractor. *Biosystems Engineering, 83*, 55–65. http://dx.doi.org/10.1006/bioe.2002.0099.

Lutz, A. E., Larson, R. S., & Keller, J. O. (2002). Thermodynamic comparison of fuel cells to the Carnot cycle. *International Journal of Hydrogen Energy, 27*, 1103–1111. http://dx.doi.org/10.1016/S0360-3199(02)00016-2.

Montalvo, M., Guerrero, J. M., Romeo, J., Emmi, L., Guijarro, M., & Pajares, G. (2013). Automatic expert system for weeds/crops identification in images from maize fields. *Expert Systems with Applications, 40*, 75–82. http://dx.doi.org/10.1016/j.eswa.2012.07.034.

Mousazadeh, H., Keyhani, A., Javadi, A., Mobli, H., Abrinia, K., & Sharifi, A. (2010). Evaluation of alternative battery technologies for a solar assist plug-in hybrid electric tractor. *Transportation Research Part D: Transport and Environment, 15*, 507–512. http://dx.doi.org/10.1016/j.trd.2010.05.002.

Mousazadeh, H., Keyhani, A., Javadi, A., Mobli, H., Abrinia, K., & Sharifi, A. (2011). Life-cycle assessment of a solar assist plug-in hybrid electric tractor (SAPHT) in comparison with a conventional tractor. *Energy Conversion and Management, 52*, 1700–1710. http://dx.doi.org/10.1016/j.enconman.2010.10.033.

Mulloney, J. A., Jr. (1993). Mitigation of carbon dioxide releases from power production via "sustainable agri-power": the synergistic combination of controlled environmental agriculture (large commercial greenhouses) and disbursed fuel cell power plants. Energy conversion and management. In *Proceedings of the International Energy Agency Carbon Dioxide Disposal Symposium 34* (pp. 913–920). http://dx.doi.org/10.1016/0196-8904(93)90036-A.

Offer, G. J., Howey, D., Contestabile, M., Clague, R., & Brandon, N. P. (2010). Comparative analysis of battery electric, hydrogen fuel cell and hybrid vehicles in a future sustainable road transport system. *Energy Policy, 38*, 24–29. http://dx.doi.org/10.1016/j.enpol.2009.08.040.

Peltre, C., Nyord, T., Bruun, S., Jensen, L. S., & Magid, J. (2015). Repeated soil application of organic waste amendments reduces draught force and fuel consumption for soil tillage. *Agriculture Ecosystems & Environment, 211*, 94–101. http://dx.doi.org/10.1016/j.agee.2015.06.004.

PVGIS - Photovoltaic Geographical Information System [WWW Document], JRCs Inst. Energy Transp. - PVGIS - Eur. Comm. URL http://re.jrc.ec.europa.eu/pvgis/(accessed 5.4.15).

RHEA Project - EU [WWW Document], "Robot Fleets Highly Eff. Agric. For. Manag. URL http://www.rhea-project.eu/(accessed 3.30.15).

Sarri, D., Lisci, R., Rimediotti, M., & Vieri, M. (2014). RHEA airblast sprayer: calibration indexes of the airjet vector related to canopy and foliage characteristics. In *Second International Conference on Robotics and Associated High-Technologies and Equipment for Agriculture and Forestry. Presented at the New trends in mobile robotics, perception and actuation for agriculture and forestry* (pp. 73–81). Madrid, Spain: PGM.

Soni, P., Taewichit, C., & Salokhe, V. M. (2013). Energy consumption and CO2 emissions in rainfed agricultural production systems of Northeast Thailand. *Agricultural Systems, 116*, 25–36. http://dx.doi.org/10.1016/j.agsy.2012.12.006.

TCS Micropumps [WWW Document], High Perform. Miniat. Pumps. URL http://www.micropumps.co.uk/(accessed 28.4.15).

Titan Enterprises Ltd - Titan flow meters for oil, boiler and diesel fuel applications - PD400 oil flowmeter [WWW Document], 2014. URL http://www.flowmeters.co.uk/pd_pd400om.php#data (accessed 20.2.15).

Tropical [WWW Document], Fuel Cell Power Gener. Hydrog. Technol. Electr. Automob. – Trop. SA Fuel Cell Hydrog. Technol. URL http://www.tropical.gr/index.php (accessed 24.4.15).